ACS APPLIED MATERIALS & INTERFACES

Letter

www.acsami.org

Photocurrent Generation in Organic Photodetectors with Tailor-Made Active Layers Fabricated by Layer-by-Layer Deposition

Benjamin Vonhoeren,[†,‡] Simon Dalgleish,[†] Laigui Hu,[†] Michio M. Matsushita,[†] Kunio Awaga,*[,†] and Bart Jan Ravoo*[,‡]

[†]Department of Chemistry and Research Centre for Materials Science, Nagoya University, Furo-cho, Chikusa, 464-8602 Nagoya, Japan

[‡]Organic Chemistry Institute, Westfälische Wilhelms-Universität Münster, Corrensstrasse 40, 48149 Münster, Germany

Supporting Information

ABSTRACT: Photodetectors supply an electric response when illuminated. The detectors in this study consist of an active layer and a polyvinylidene fluoride (PVDF) blocking layer, which are sandwiched by an aluminum and an indium tin oxide (ITO) electrode. The active layer was prepared of Zn porphyrins and assembled by covalent layer-by-layer (LbL) deposition. Layer growth was monitored by UV−vis absorbance, ellipsometry, and X-ray photoelectron spectroscopy. Upon exposure to chopped light, the detectors show an alternating transient photocurrent, which is limited by the accumulation of space charges at the blocking layer/active layer interface. We could show that the number of photoactive layers has a significant impact on device performance. The fastest response was achieved with fewer layers. The highest photocurrents were measured for detectors with an intermediate number of layers, beyond which, more layers did not lead to an increase in the photocurrent despite containing more active material.

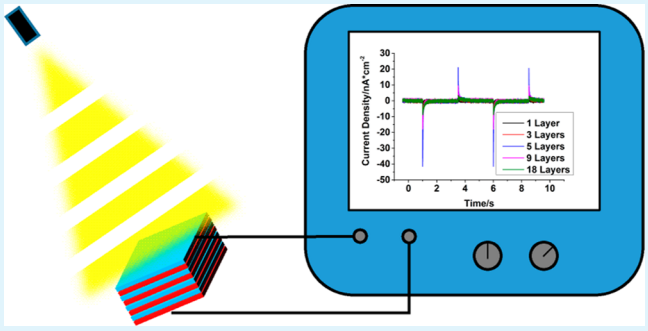

KEYWORDS: *organic electronics, layer-by-layer deposition, photocurrent, porphyrin, photodetector, active layer*

The layer-by-layer (LbL) synthesis of nanostructured materials has attracted much attention because of its simplicity, controllability, universality, and capacity for multicomponent architecture.[1−3] Indeed, this method does not require any special equipment; tweezers and beakers are sufficient to deposit organic layers with well-defined thicknesses ranging from sub nanometer to several nanometers. Early examples of the LbL method relied on electrostatic interactions.[3] Later, covalently bound multilayers were introduced, which demonstrated enhanced stability.[4] The, "click" reactions, such as azide−alkyne cycloaddition[5−7] and thiol−ene addition,[8,9] are particularly suitable for multilayer assembly as they proceed in high yield with small amounts of side-products under mild conditions.[10]

The functional properties of nanolayered materials obtained by LbL methods are promising in various fields involving physics, chemistry, and biology.[1] The stepwise increase in the absorption intensity with an increase in layer number is the most visible and simple example demonstrating the usefulness of the LbL method for making well-defined nanolayered structures. This method has been used for the assembly of functional materials for capacitors,[11,12] batteries,[13] and organic field-effect transistors.[14]

Optoelectronic devices, such as solar cells, photodetectors, and light emitting diodes, play an important role in our daily lives. The development of organic optoelectronic devices, in which traditional inorganic semiconductors are substituted by organic materials, has attracted growing attention among material scientists.[15] Although they cannot compete with traditional semiconductor devices in terms of efficiency or long-term stability, they are superior to inorganic devices in a number of respects: targeted wavelength modifications, flexible architectures, and low production costs. Recently, LbL structures were implemented in optoelectronic devices for the preparation of organic solar cells[16−18] and dye-sensitized solar cells (DSSCs).[19,20] The recent study by Dinolfo et al. is particularly interesting because in this study we employed the same LbL approach to assemble the active material.[20] Their study focused on the performance of DSSCs in terms of power conversion efficiency and short-circuit currents, which were found to be optimal at an intermediate layer thickness.

Organic photodetectors, which are important in the fields of imaging and data transfer, have attracted less attention even though they show similar benefits.[21−25] In 2010, Hu et al. reported a new type of organic photodetector that consists of an active layer and a blocking layer that are sandwiched by an indium tin oxide (ITO) and Al electrode.[26] Because of the

Received: December 22, 2014
Accepted: March 23, 2015
Published: March 23, 2015

DOI: 10.1021/am509031u
ACS Appl. Mater. Interfaces 2015, 7, 7049−7053

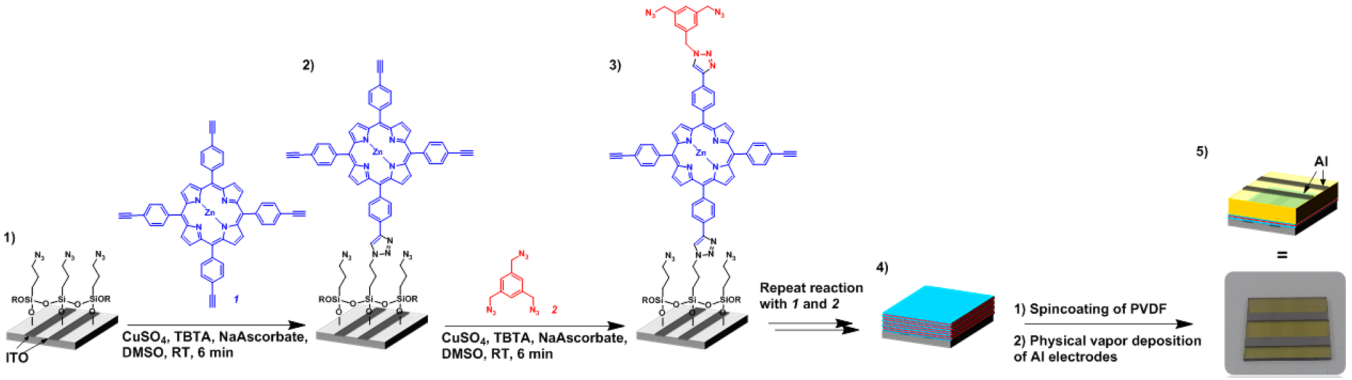

Figure 1. Device assembly by the layer-by-layer (LbL) technique on an azide-functionalized self-assembled monolayer. TBTA: tris(benzyltriazolylmethyl)amine, PVDF: polyvinylidene fluoride.

presence of a thick blocking layer, an illumination period induces a pair of positive and negative transient currents at the beginning and end of the illumination, respectively, such that an alternating transient photocurrent could be detected upon exposure to chopped light. Thus, such devices are capable of periodic light detection, which is important in signal transfer.

In this contribution, we show that the active layer of organic photodetectors can be easily assembled by the LbL method without the need for special instruments. We prepared a series of samples with active layer thicknesses ranging from 3 to 45 nm deposited by the layer-by-layer method on ITO with Zn porphyrin as the active material, following the procedure described by Dinolfo et al.[6,20] Polyvinylidene fluoride (PVDF) was chosen as the blocking layer and Al as the top electrode. The layer growth was monitored by ellipsometry, UV−vis absorbance, and X-ray photoelectron spectroscopy (XPS). Transient photocurrents were measured upon exposure to chopped light. It could be shown that the layer number has a pronounced effect on signal intensity and shape.

We prepared nine devices with active layers of varying layer number on patterned ITO substrates using the LbL method. In detail, the patterned ITO substrates were first cleaned by sonication for 3 min in dichloromethane, acetone, ethanol, and water and then activated in a mixture of H_2O:NH_3(aq):H_2O_2(aq) (5:1:1 volume fractions) to increase the density of hydroxyl functions on the surface. The activated surfaces were then immersed in a solution of (3-bromopropyl)-trichlorosilane in toluene for 15 min to give self-assembled monolayers that bear terminal bromides. Although longer alkyl chains usually result in monolayers of higher ordering, we chose propyl silane to facilitate charge transport to the ITO electrode. An increase in the contact angle from <10° for the activated surface to 70° (see Figure S3, Supporting Information (SI)) and the appearance of a Br signal in the X-ray photoelectron spectrum (see Figure S4, SI) confirmed successful deposition. Next, the terminal bromides were substituted with azides by heating the monolayers at 80 °C in a saturated solution of sodium azide in dimethylformamide for 2 days to yield the desired azide terminated monolayers (Figure 1.1). The substitution was analyzed by X-ray photoelectron spectroscopy (see Figure S4, SI), finding that the Br signal vanished and a N signal emerged with two peaks at 400 and 405 eV, which are characteristic of azides.[27]

These azide-terminated self-assembled monolayers were immersed in a solution of porphyrin **1**. The surface-bound azides reacted with the alkyne groups of the porphyrin in a Cu-catalyzed azide−alkyne click reaction[6,28] to yield samples covered with a single layer of porphyrin (Figure 1.2). In a subsequent reaction, the unreacted alkynes of the porphyrin molecules reacted with the aromatic triazide **2** to give azide terminated surfaces (Figure 1.3). This cycle was repeated until the desired number of layers were assembled (Figure 1.4). A tetra-substituted porphyrin and a tris-substituted azide were used to ensure a high density of functional groups on the uppermost layer. Disubstituted molecules were not used in this study due to the risk that they may bind with both groups to the previous layer, which would result in decreased functionality with increasing layer number.[9] As a consequence, layer growth would then be nonlinear.

Figure 2 illustrates results of UV−vis absorbance, ellipsometry, and XPS measurements. The UV−vis absorption peaks of the porphyrin molecules at 440 nm (Figure 2A) scale almost linearly with the number of porphyrin layers (Figure 2B, red triangles), which indicates that the same amount of porphyrin is deposited with each immersion. The peak maxima of the immobilized porphyrins are broadened and shifted to higher wavelengths compared to the solution spectra (λ_{max} = 422 nm, not shown), which suggest a significant degree of porphyrin aggregation as a result of π-π stacking.[6]

The thickness of the active layer was first determined by ellipsometry (Figure 2B, black squares). We measured samples from 1 to 18 layers, but only obtained reliable data for the thinnest layers. The model analysis with an iterative procedure did not lead to reasonable thicknesses for samples with more than five layers. The ellipsometry measurements were validated by angle-resolved XPS measurements (Figure 2B, blue squares). As the absorbance increases linearly, it can be assumed that the thickness increases in a linear fashion as well. The average thickness of one bilayer was 3 nm. The atomic composition of the samples was measured by XPS. Characteristic peaks for C, N, and Zn could be detected (see Figure S5, SI). Some of the Cu catalyst remained entrapped in the active layer. The signal intensities for N and Zn increased with layer number. The increase of the N peak at 400 eV is characteristic for the triazole that is formed during the reaction.[27] The intensity of the N peak at 405 eV, which derives from residual unreacted azides, increases much more slowly. As a consequence, the ratio of these two peaks is higher than the 2:1 that would be expected for unreacted azides and proves that the molecules are covalently bound to the substrate. The alternating ratio of Zn to N provided further evidence for the layered structure of the active material (Figure 2C), because the

DOI: 10.1021/am509031u
ACS Appl. Mater. Interfaces 2015, 7, 7049−7053

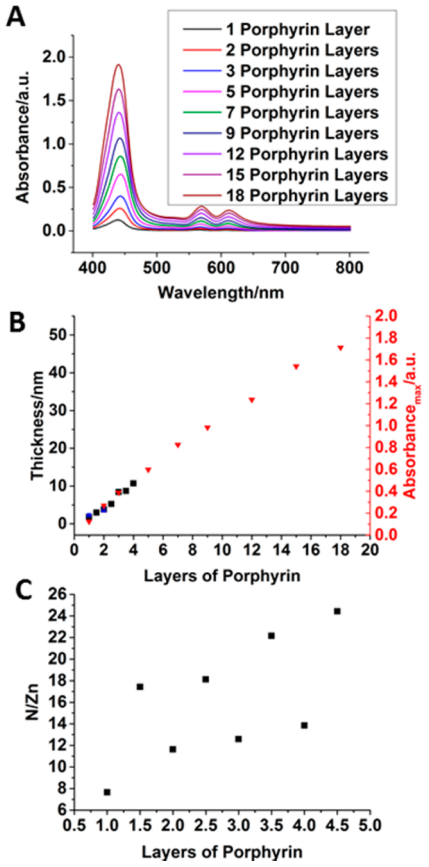

Figure 2. Analysis of LbL deposition of Zn porphyrin by (A) absorbance spectra and (B) absorbance$_{max}$ as a function of layer number (red triangles) with thickness as a function of layer number derived from ellipsometry measurements (black squares) and angle-resolved XPS (B, blue squares). (C) Ratio of N to Zn derived from XPS measurements; samples with *n* layers of porphyrin are porphyrin terminated whereas samples with *n*.5 layers bear a terminal azide layer.

intensities for elements in the uppermost layer show the highest intensities in the XPS spectra. Note that samples with *n* layers of porphyrin are porphyrin terminated whereas samples with *n*.5 layers terminate with an azide layer.

Polyvinylidene difluoride (PVDF) was chosen as the blocking layer due to its high dielectric constant, which has previously been shown to improve the photocurrent response for devices of this structure.[26] PVDF spin-coated from 2-butanone gave films with an average thickness of 300 nm (Figure 1.5), as determined by surface profilometry. Two aluminum counter electrodes with a thickness of 100 nm, estimated by quartz crystal microbalance, were deposited orthogonal to the underlying ITO electrodes by physical vapor deposition (Figure 1.5). This device architecture allowed us to measure each sample on four different spots, where ITO and aluminum electrodes lie on top of each other with an overlap area of 4 mm^2.

To analyze optoelectronic properties of the devices, the active areas were exposed to square-wave modulated light from a blue LED (frequency = 0.2 Hz, λ_{max} = 427 nm) controlled by a function generator (Tektronix AFG320) under ambient conditions and illuminating through the ITO. The resulting photocurrents were amplified a by low-noise trans-impedance amplifier (Femto DLPCA 200) and were recorded on an oscilloscope (Tektronix TDS5104B). The ITO electrode was grounded, and an additional bias voltage was not applied to the device. The active material consists of a p-type organic semiconductor.[20]

All samples showed a negative transient photocurrent upon exposure to light (Figure 3A and B), suggesting that holes were

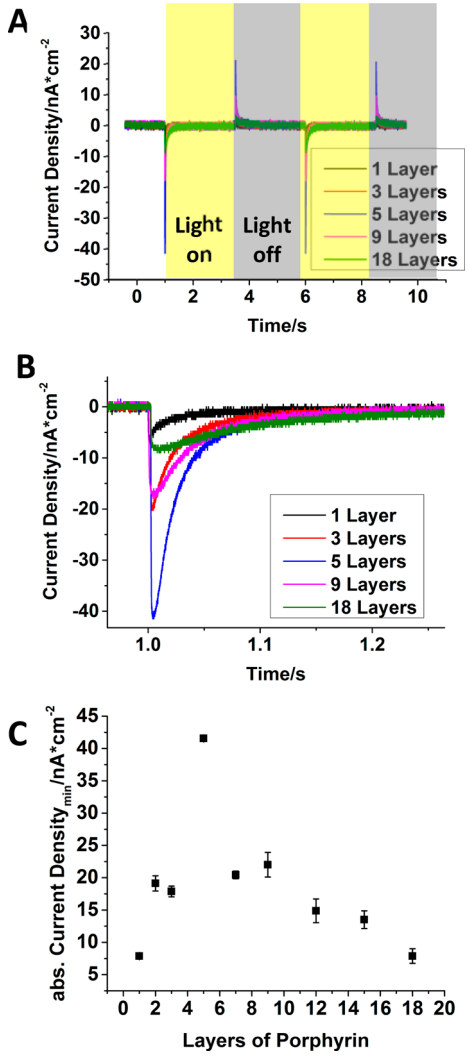

Figure 3. (A) Photoresponse of samples with active layers of different layer numbers under illumination with chopped light at a wavelength of 427 nm. (B) Amplification of the negative transient photocurrents. (C) Absolute current density as a function of the number of layers. Error bars indicate the deviation between four different spots on the same sample.

extracted at the ITO electrode. A positive transient current was observed when the light was switched off. The photoresponse remained relatively stable over hundreds of cycles (35% decrease in current intensity after 3 h of continuous irradiation, see Figure S6, SI). Because the devices were tested in air, the decrease in signal intensity is most likely due to the effect of atmospheric contaminants on the active material under illumination. Figure 3C charts the trend in the photocurrent maximum with an increasing number of layers. The magnitude of the transient photocurrent response depends strongly on the number of photoactive layers deposited. It can be seen that even a single layer of porphyrin molecules can generate a measurable photocurrent (Figure 3B, black line). This sample showed the fastest response (i.e., the narrowest signal). In this

DOI: 10.1021/am509031u
ACS Appl. Mater. Interfaces 2015, 7, 7049−7053

batch, the maximal photocurrent increased for samples up to five layers, which could be attributed to the higher amount of porphyrin in the active layer available to contribute to absorption and charge separation (Figure 3C). Beyond five layers, both the rise and decay times increased, which resulted in a broadened photocurrent signal (Figure 3B) and a drop in the photocurrent maximum despite the higher amount of active material in these samples.

To test the reproducibility of devices prepared by this method, we prepared three additional batches in which we consistently observed the same trends in maximal photocurrent and signal shape (see Figure S7, SI). Within these batches, the maximal photocurrent was obtained for samples with three to nine layers. These deviations may be caused by three factors. First, the reproducibility of the LbL deposition is not perfect, as shown by UV−vis absorbance (see Figure S7, SI). LbL assemblies based on covalent reactions yield multilayers with enhanced stability compared to LbL assemblies based on hydrogen bonding or electrostatic interactions. Nevertheless, one disadvantage of covalent LbL is its irreversible character. Once a molecule has reacted, it cannot be removed from the surface. In contrast, LbL based on noncovalent interactions is more dynamic, and rearrangements during the LbL process are therefore more likely, which can result in enhanced order within the layers. LbL by covalent bonding could lead to sublayer coverage, which would have an effect on layer density and layer thickness, especially for multilayer films. Second, the amount of Cu catalyst that remained entrapped within the active layer may vary between batches (see Figure S5, SI). Because Cu may decrease the exciton diffusion length, the Cu concentration will likely affect the device efficiency. Third, the morphology of the spin-coated PVDF depends strongly on the batch due to the strong tendency of PVDF to crystallize. This would have a significant effect on the thickness of the PVDF layer as well as the electrode area.

Despite these deviations between batches, the same trend in photoresponse could be observed in each case. Increasing the layer number results in the maximum photocurrent first increasing and then dropping for thicker active layers, and the signal broadened with increasing layer number.

We propose the following simplified mechanism, which can be compared to the five-step process in binary donor−acceptor photovoltaic cells[15] to explain photocurrent generation and layer dependency: (1) absorption of photons and the formation of excitons in the active layer; (2) diffusion of the excitons to the semiconductor/blocking layer interface, where the electric field is large enough to separate the exciton into free charges; (3) separation of the excitons into holes and electrons at the interface; (4) drift of the holes to the ITO electrode and accumulation of the electrons at the blocking layer, and (5) collection of holes at the ITO electrode. The distances that need to be overcome by the excitons and free charge carriers are small in photodetectors with thin active layers, which leads to narrow signals. Moreover, exciton recombination or charge trapping is less likely than in thicker layers in which excitons and free carriers have to travel longer distances to produce a measurable photocurrent.

The photodetectors studied in this work differ from the DSSCs of Dinolfo et al. in terms of device architecture and the mechanism of photocurrent generation. Nevertheless, they both show that devices with an intermediate thickness are the most efficient. Increased probabilities of charge trapping and recombination processes in thicker devices outweigh the higher amount of active material.

In conclusion, we prepared organic photodetectors with an active layer of porphyrins assembled by covalent LbL deposition and showed that the number of photoactive layers had an impact on the performance of the photodetector. Photodetectors could be fabricated with a single molecular layer of porphyrin. However, detectors with an intermediate number of layers gave the highest photocurrents, and device efficiency decreased with additional layers, which also showed a slower response. The two primary findings of this study are that the LbL method is well suited for fabricating organic photodetectors with controlled chromophore content and that the number of active layers has a critical impact on device performance. We are currently further investigating the thickness dependence to develop a better understanding of the mechanism of charge separation and photocurrent generation.

■ ASSOCIATED CONTENT

Ⓢ Supporting Information

Synthetic procedures, description of SAM preparation, LbL deposition, and further analytical results. This material is available free of charge via the Internet at http://pubs.acs.org.

■ AUTHOR INFORMATION

Corresponding Authors

*E-mail: awaga@mbox.chem.nagoya-u.ac.jp.
*E-mail: b.j.ravoo@uni-muenster.de.

Notes

The authors declare no competing financial interest.

■ ACKNOWLEDGMENTS

This work was supported by the Deutsche Forschungsgemeinschaft (DFG, IRTG 1143 Münster−Nagoya). We thank Siltronic AG for the donation of silicon wafers.

■ ABBREVIATIONS

DSSC, dye-sensitized solar cell
ITO, indium tin oxide
LbL, layer-by-layer
PVDF, polyvinylidene fluoride
TBTA, tris(benzyltriazolylmethyl)amine
XPS, X-ray photoelectron spectroscopy

■ REFERENCES

(1) Ariga, K.; Yamauchi, Y.; Rydzek, G.; Ji, Q.; Yonamine, Y.; Wu, K. C.-W.; Hill, J. P. Layer-by-Layer Nanoarchitectonics: Invention, Innovation, and Evolution. *Chem. Lett.* **2014**, *43*, 36−68.

(2) Zhang, X.; Chen, H.; Zhang, H. Layer-by-Layer Assembly: From Conventional to Unconventional Methods. *Chem. Commun.* **2007**, 1395−1405.

(3) Decher, G. Fuzzy Nanoassemblies: Toward Layered Polymeric Multicomposites. *Science* **1997**, *277*, 1232−1237.

(4) Bergbreiter, D. E.; Liao, K.-S. Covalent Layer-by-Layer Assembly—an Effective, Forgiving Way to Construct Functional Robust Ultrathin Films and Nanocomposites. *Soft Matter* **2009**, *5*, 23−28.

(5) Such, G. K.; Quinn, J. F.; Quinn, A.; Tjipto, E.; Caruso, F. Assembly of Ultrathin Polymer Multilayer Films by Click Chemistry. *J. Am. Chem. Soc.* **2006**, *128*, 9318−9319.

(6) Palomaki, P. K. B.; Dinolfo, P. H. A Versatile Molecular Layer-by-Layer Thin Film Fabrication Technique Utilizing Copper(I)-Catalyzed Azide−Alkyne Cycloaddition. *Langmuir* **2010**, *26*, 9677−9685.

DOI: 10.1021/am509031u
ACS Appl. Mater. Interfaces 2015, 7, 7049−7053

(7) Rydzek, G.; Terentyeva, T. G.; Pakdel, A.; Golberg, D.; Hill, J. P.; Ariga, K. Simultaneous Electropolymerization and Electro-Click Functionalization for Highly Versatile Surface Platforms. *ACS Nano* **2014**, *8*, 5240−5248.
(8) Li, Y.; Wang, D.; Buriak, J. M. Molecular Layer Deposition of Thiol−Ene Multilayers on Semiconductor Surfaces. *Langmuir* **2010**, *26*, 1232−1238.
(9) Schulz, C.; Nowak, S.; Fröhlich, R.; Ravoo, B. J. Covalent Layer-by-Layer Assembly of Redox Active Molecular Multilayers on Silicon (100) by Photochemical Thiol-Ene Chemistry. *Small* **2012**, *8*, 569−577.
(10) Kolb, H. C.; Finn, M. G.; Sharpless, K. B. Click Chemistry: Diverse Chemical Function from a Few Good Reactions. *Angew. Chem., Int. Ed.* **2001**, *40*, 2004−2021.
(11) Lee, S. W.; Kim, J.; Chen, S.; Hammond, P. T.; Shao-Horn, Y. Carbon Nanotube/Manganese Oxide Ultrathin Film Electrodes for Electrochemical Capacitors. *ACS Nano* **2010**, *4*, 3889−3896.
(12) Li, Z.; Wang, J.; Liu, X.; Liu, S.; Ou, J.; Yang, S. Electrostatic Layer-by-Layer Self-Assembly Multilayer Films Based on Graphene and Manganese Dioxide Sheets as Novel Electrode Materials for Supercapacitors. *J. Mater. Chem.* **2011**, *21*, 3397−3403.
(13) Lee, S. W.; Yabuuchi, N.; Gallant, B. M.; Chen, S.; Kim, B.-S.; Hammond, P. T.; Shao-Horn, Y. High-Power Lithium Batteries from Functionalized Carbon-Nanotube Electrodes. *Nat. Nanotechnol.* **2010**, *5*, 531−537.
(14) Li, H.; Pang, S.; Wu, S.; Feng, X.; Müllen, K.; Bubeck, C. Layer-by-Layer Assembly and UV Photoreduction of Graphene−Polyoxometalate Composite Films for Electronics. *J. Am. Chem. Soc.* **2011**, *133*, 9423−9429.
(15) Sun, S.-S., Dalton, L. R., Eds. *Introduction to Organic Electronic and Optoelectronic Materials and Devices*, 1st ed; CRC Press: Boca Raton, USA, 2008.
(16) Hsu, C.-L.; Lin, C.-T.; Huang, J.-H.; Chu, C.-W.; Wei, K.-H.; Li, L.-J. Layer-by-Layer Graphene/TCNQ Stacked Films as Conducting Anodes for Organic Solar Cells. *ACS Nano* **2012**, *6*, 5031−5039.
(17) Wang, Y.; Tong, S. W.; Xu, X. F.; Özyilmaz, B.; Loh, K. P. Interface Engineering of Layer-by-Layer Stacked Graphene Anodes for High-Performance Organic Solar Cells. *Adv. Mater.* **2011**, *23*, 1514−1518.
(18) Li, M.; Ishihara, S.; Akada, M.; Liao, M.; Sang, L.; Hill, J. P.; Krishnan, V.; Ma, Y.; Ariga, K. Electrochemical-Coupling Layer-by-Layer (ECC−LbL) Assembly. *J. Am. Chem. Soc.* **2011**, *133*, 7348−7351.
(19) Chen, P.-Y.; Ladewski, R.; Miller, R.; Dang, X.; Qi, J.; Liau, F.; Belcher, A. M.; Hammond, P. T. Layer-by-Layer Assembled Porous Photoanodes for Efficient Electron Collection in Dye-Sensitized Solar Cells. *J. Mater. Chem. A* **2013**, *1*, 2217−2224.
(20) Palomaki, P. K. B.; Civic, M. R.; Dinolfo, P. H. Photocurrent Enhancement by Multilayered Porphyrin Sensitizers in a Photoelectrochemical Cell. *ACS Appl. Mater. Interfaces* **2013**, *5*, 7604−7612.
(21) Baeg, K.-J.; Binda, M.; Natali, D.; Caironi, M.; Noh, Y.-Y. Organic Light Detectors: Photodiodes and Phototransistors. *Adv. Mater.* **2013**, *25*, 4267−4295.
(22) Peumans, P.; Yakimov, A.; Forrest, S. R. Small Molecular Weight Organic Thin-Film Photodetectors and Solar Cells. *J. Appl. Phys.* **2003**, *93*, 3693−3723.
(23) Leung, S.-F.; Zhang, Q.; Xiu, F.; Yu, D.; Ho, J. C.; Li, D.; Fan, Z. Light Management with Nanostructures for Optoelectronic Devices. *J. Phys. Chem. Lett.* **2014**, *5*, 1479−1495.
(24) Dong, H.; Zhu, H.; Meng, Q.; Gong, X.; Hu, W. Organic Photoresponse Materials and Devices. *Chem. Soc. Rev.* **2012**, *41*, 1754−1808.
(25) Tedde, S. F.; Kern, J.; Sterzl, T.; Fürst, J.; Lugli, P.; Hayden, O. Fully Spray Coated Organic Photodiodes. *Nano Lett.* **2009**, *3*, 980−983.
(26) Hu, L.; Noda, Y.; Ito, H.; Kishida, H.; Nakamura, A.; Awaga, K. Optoelectronic Conversion by Polarization Current, Triggered by Space Charges at Organic-Based Interfaces. *Appl. Phys. Lett.* **2010**, *96*, 243303−243304.
(27) Wendeln, C.; Singh, I.; Rinnen, S.; Schulz, C.; Arlinghaus, H. F.; Burley, G. A.; Ravoo, B. J. Orthogonal, Metal-Free Surface Modification by Strain-Promoted Azide−alkyne and Nitrile Oxide−alkene/alkyne Cycloadditions. *Chem. Sci.* **2012**, *3*, 2479−2484.
(28) Evans, R. A. The Rise of Azide−Alkyne 1,3-Dipolar "Click" Cycloaddition and Its Application to Polymer Science and Surface Modification. *Aust. J. Chem.* **2007**, *60*, 384−395.

DOI: 10.1021/am509031u
ACS Appl. Mater. Interfaces 2015, 7, 7049−7053